SCIENTIFIC REPORTS

OPEN

SUBJECT AREAS:
ELECTROCHEMISTRY
MATERIALS CHEMISTRY
INORGANIC CHEMISTRY
GREEN CHEMISTRY

Received
12 June 2012

Accepted
8 August 2012

Published
24 August 2012

Correspondence and requests for materials should be addressed to N.M. (tmizuno@mail.ecc.u-tokyo.ac.jp)

Oxygen rocking aqueous batteries utilizing reversible *topotactic* oxygen insertion/extraction in iron-based perovskite oxides $Ca_{1-x}La_xFeO_{3-\delta}$

Mitsuhiro Hibino, Takeshi Kimura, Yosuke Suga, Tetsuichi Kudo & Noritaka Mizuno

Department of Applied Chemistry, School of Engineering, The University of Tokyo, 7-3-1 Hongo, Bunkyo-ku, Tokyo, 113-8656, JAPAN.

Developments of large-scale energy storages with not only low cost and high safety but also abundant metals are significantly demanded. While lithium ion batteries are the most successful method, they cannot satisfy all conditions. Here we show the principle of novel lithium-free secondary oxygen rocking aqueous batteries, in which oxygen shuttles between the cathode and anode composed of iron-based perovskite-related oxides $Ca_{0.5}La_{0.5}FeO_z$ ($2.5 \leq z \leq 2.75$ and $2.75 \leq z \leq 3.0$). Compound $Ca_{0.5}La_{0.5}FeO_z$ can undergo two kinds of reduction and reoxidation of Fe^{4+}/Fe^{3+} and Fe^{3+}/Fe^{2+}, that are accompanied by reversible and repeatable *topotactic* oxygen extraction and reinsertion during discharge and charge processes.

Lithium ion batteries (LIBs) based on rocking lithium between cathode and anode electrodes are used in a wide range of applications from portable electronics to vehicle propulsion. However, there are cost and resource problems since most LIBs use not only expensive lithium but also less abundant metals such as cobalt. In addition, use of flammable organic electrolyte solutions may cause a safety problem. Those problems are critical especially for large-scale batteries used for electric vehicles and electric grids. Some alternatives have recently been proposed by the replacement of lithium and cobalt-based oxides with sodium and iron-based compounds, respectively: For example, Ellis et al.[1] have shown the viability of sodium-ion batteries utilizing a sodium iron fluorophosphate (Na_2FePO_4F) as a cathode material, where reversible redox of iron (Fe^{2+}/Fe^{3+}) proceeds with topotactic extraction and reinsertion of sodium in organic electrolyte solutions. More recently, Wessells et al.[2] have reported that aqueous sodium ion batteries employing a Prussian blue analogue of a nickel hexacyanoferrate $A_xNi_yFe(CN)_6 \cdot nH_2O$ (A: alkali metal ions) as an intercalation cathode are attractive for grid-scale power storage. Batteries using aqueous electrolytes have advantages in terms of safety and cost in addition to lithium-free, while they do not show high cell voltages due to potential window of water. In addition, large-scale energy storage is needed more and more today. Therefore, it is urgent to develop novel batteries satisfying not only cost and safety but also "element strategy[3]" requirements.

It is well known that some kinds of perovskite-type oxides of $A_{1-x}Sr_xCoO_3$ (A=La or Nd) show good oxygen diffusivity[4,5] and the oxygen atoms of such compounds can be extracted and reinserted topotactically by electrochemical reduction and reoxidation in an aqueous alkaline solution[6,7]. Longo et al. have reported that $CaMnO_3$ electrochemically undergoes extraction and reinsertion of oxygen in a strong basic solution and that this reaction can be applied to cathode materials[8].

Electrochemical oxidation and reduction (Fe^{4+}/Fe^{3+}) of $Sr_{1-x}La_xFeO_z$ in an alkaline solution reversibly take place at least on the surface in the range $2.5 + x/2 < z < 3$[9], while the iron valences can possibly be changed from $3 - x$ to 3 in the oxygen composition range $2.5 < z < 2.5 + x/2$. Therefore, we have reached an idea that compounds $A_{1-x}La_xFeO_z$ (A = Ca, Sr) can work as not only a cathode but also an anode utilizing different oxygen composition ranges of the $Fe^{3+}/Fe^{4+}$and Fe^{2+}/Fe^{3+} couples, respectively.

In this report, we show the principle of novel lithium-free secondary oxygen rocking batteries, in which oxygen shuttles between the cathode and anode composed of iron-based perovskite-related oxides $Ca_{0.5}La_{0.5}FeO_z$ ($2.5 \leq z \leq 2.75$ and $2.75 \leq z \leq 3.0$) by utilizing *topotactic* oxygen extraction and reinsertion during discharge and charge processes (Fig. 1).

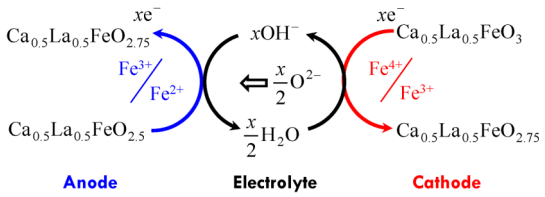

Figure 1 | Operating principle of oxygen rocking batteries using CLFO. This is an example of oxygen rocking batteries. The directions of arrows indicate discharging. In discharging, cathode and anode materials undergo oxygen extraction and insertion, respectively, and oxygen is transferred from the cathode to the anode in an electrolyte.

Results

Electrochemical behaviors of $Ca_{0.5}La_{0.5}FeO_z$. Figure 2 illustrates the potential variation of $Ca_{0.5}La_{0.5}FeO_z$ (CLFO) at a constant current of 1.40 mA g^{-1}. Since the composition of the as-synthesized sample was determined to be $Ca_{0.5}La_{0.5}FeO_{2.863}$, the electrochemical measurement was started from $z = 2.863$ as denoted by the initial state. In the oxidation process, the potential gradually increased and reached a plateau (ca. 0.5 V) below $z = 3$ due to oxygen evolution. On the other hand, in the reduction process, the potential gradually decreased around 0 V, steeply decreased from −0.1 V to −0.8 V around $z = 2.75$, gradually decreased around −0.9 V and then leveled off around −1.1 V due to hydrogen evolution.

Changes in crystal structures and valence states of iron with electrochemical reduction. Figure 3 shows X-ray diffraction (XRD) patterns of the CLFO samples prepared by electrochemical-reduction shown by the circles in Fig. 2. All peaks of $Ca_{0.5}La_{0.5}FeO_{2.863}$ were assignable to the $GdFeO_3$-type structure, which is slightly-distorted cubic. The Rietveld analysis successfully provided the cell parameters and atomic positions with small value of goodness-of-fit of 1.54 (see Fig. S1 and the refined parameters were shown in Supplementary information). The unit cell could be regarded as pseudo-cubic (Fig. 3). Upon the reduction of $Ca_{0.5}La_{0.5}FeO_{2.863}$, neither new peak nor peak-splitting was observed except for lower angle shifts of peak positions, showing the expansion of the cell parameter of a^*_{cubic}. The a^*_{cubic} values are plotted as a function of oxygen contents in Fig. 4. They

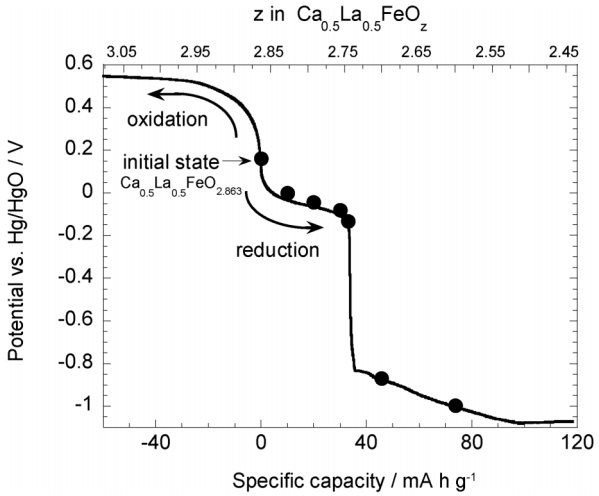

Figure 2 | Potential variation of $Ca_{0.5}La_{0.5}FeO_{2.863}$ in the oxidation and reduction at a constant current of 1.40 mA g^{-1}. The upper transversal axis indicates the oxygen contents (z) electrochemically estimated with integrated currents assuming the following reaction, $Ca_{0.5}La_{0.5}FeO_{2.863} + \delta H_2O + 2\delta e^- \rightleftarrows Ca_{0.5}La_{0.5}FeO_{2.863-\delta} + 2\delta OH^-$.

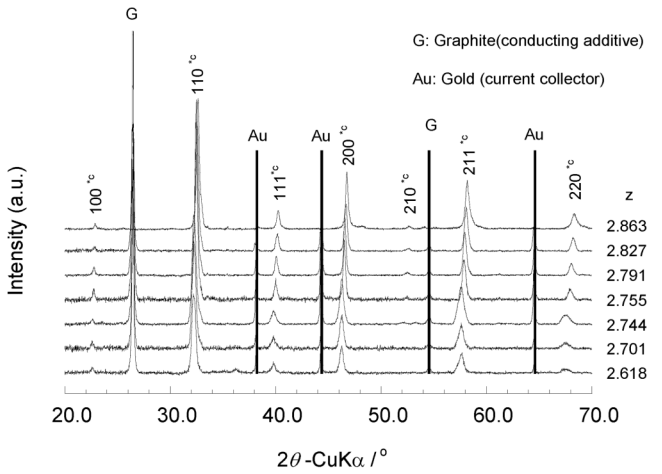

Figure 3 | XRD profiles of electrochemically reduced CLFO. The *hkl* indices assigned to the cubic cells with the reduced-cell parameter, a^*_{cubic} ($a \approx 2^{1/2} \times a^*_{cubic}$, $b \approx 2 \times a^*_{cubic}$, $c \approx 2^{1/2} \times a^*_{cubic}$; a, b, c: cell parameters based on $GdFeO_3$-type structure) were shown. z; see the caption note of Fig. 2.

increased with decrease in z from 2.863 to 2.744 and did not much change below $z = 2.744$.

Mössbauer parameters of CLFO samples ($z = 2.744$, 2.701, and 2.618) are summarized in Table 1.

Repeatability of Electrochemical reaction of CLFO. As shown in Fig. 2, the electrochemical reduction (viz. oxygen extraction) of CLFO proceeded stepwise in two distinct potential regions around 0 V (due to Fe^{4+}/Fe^{3+}) and −0.8 V (Fe^{3+}/Fe^{2+}). To construct a rechargeable battery using CLFO, reoxidation reactions must proceed reversibly at these potential levels. Figure 5 shows the results of repeated redox tests under a constant current density of 5.60 mA g^{-1}. The electrochemical reactions in potential regions around both 0 V and −0.8 V were substantially reversible and repeatable. Especially in the higher potential region, the shapes of the reduction and oxidation curves remained almost unchanged with repetition of the cycles, and the potential difference between the reduction and oxidation processes was small.

When particles of $Ca_{0.5}La_{0.5}FeO_{2.863}$ were treated in a strong basic aqueous solution at pH 14 for 24 h, no change in the XRD pattern was observed, showing that $Ca_{0.5}La_{0.5}FeO_{2.863}$ is stable in a strong basic aqueous solution. In addition, the XRD pattern of $Ca_{0.5}La_{0.5}FeO_{2.863}$ was hardly changed and only the perovskite phase

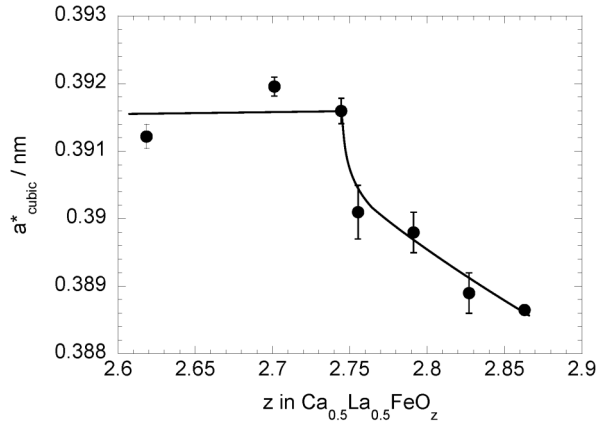

Figure 4 | The variation in cell parameters of CLFO on the basis of the pseudo-cubic cell. The estimated standard deviations were shown by lengths of bars. z; see caption note of Fig. 2.

Table 1 | Mössbauer parameters and oxygen contents estimated from valence and coordination states of iron ions in $Ca_{0.5}La_{0.5}FeO_z$

	Signal						z calculated	
z calculated with iodometric titration	IS/mm s^{-1}	QS/mm s^{-1}	H_{hf}/T	I / %	Assignment		with Fe valence	with coordination number of oxygen
	0.34(2)	0.63(4)	-	11.6(4)	Fe^{3+}			
2.744	0.400(4)	−0.095(8)	51.49(4)	69.1(8)	$Fe^{3+}_{S5/2}$	(O)	2.75	-
	0.27(3)	0.39(6)	43.1(2)	19(1)	$Fe^{3+}_{S5/2}$	(T)		
	0.226(5)	0.685(9)	-	16.0(2)	Fe^{2+}_{S0}	(O)		
	0.52(2)	−1.43(3)	24.7(1)	4.1(4)	Fe^{2+}_{S1}	(T)		
						(P)		
2.701	0.246(2)	−0.041(5)	51.99(4)	29(2)	$Fe^{3+}_{S5/2}$	(O)	2.65(4)	2.75(8)*T
	0.247(4)	−0.075(9)	49.81(9)	25(2)	$Fe^{3+}_{S5/2}$	(O)		2.73(8)*P
	0.34(2)	0.36(4)	44.4(2)	11(1)	$Fe^{3+}_{S5/2}$	(T)		
	0.08(3)	−0.68(5)	43.9(2)	14(1)	$Fe^{3+}_{S5/2}$	(T)		
	0.231(4)	0.812(7)	-	19.4(3)	Fe^{2+}_{S0}	(O)		
	0.47(2)	−1.48(7)	24.1(2)	8.0(6)	Fe^{2+}_{S1}	(T)		
						(P)		
2.618	0.246(4)	−0.098(9)	51.30(6)	19(1)	$Fe^{3+}_{S5/2}$	(O)	2.61(7)	2.62(11)*T
	0.229(6)	−0.09(1)	48.85(8)	19(2)	$Fe^{3+}_{S5/2}$	(O)		2.61(11)*P
	0.47(3)	0.33(8)	44.2(2)	17(3)	$Fe^{3+}_{S5/2}$	(T)		
	0.14(4)	−0.42(6)	44.1(2)	18(3)	$Fe^{3+}_{S5/2}$	(T)		

*Oxygen contents were calculated assuming that Fe^{2+} ions exist in either tetrahedral (T) or square-pyramidal (P) site in addition to the octahedral site.

was observed even after discharge and charge cycles. We also confirmed that the electrolyte solution was clear and no unloading of the electrode materials occurred after discharge and charge cycles.

Discussion

The oxygen contents obtained in different two ways (from (i) valence of iron and (ii) coordination number of oxygen) with Mössbauer data are also shown in Table 1. These oxygen contents were close to each other, showing that the oxygen contents in CLFO are appropriately determined. In addition, these oxygen contents agreed with those estimated electrochemically, indicating that CLFO can electrochemically be reduced with high Faradaic efficiency and that the oxygen contents are electrochemically controlled by the integrated currents.

Since the valence of the all iron ions is +3 at $z = 2.75$, Fe^{4+} ions in $Ca_{0.5}La_{0.5}FeO_{2.863}$ are probably reduced to Fe^{3+} ones around 0 V. The increase in the a^*_{cubic} values is explained by the reduction of Fe^{4+} ions to larger Fe^{3+} ones. Further electrochemical reduction would proceed by the reduction of Fe^{3+} ions to Fe^{2+} ones. The a^*_{cubic} values did not much change beyond $z = 2.744$, which is likely explained by the reduction of high-spin Fe^{3+} ions (ionic radius[10]: 79 pm) to similarly-sized low-spin Fe^{2+} ones (75 pm). The Mössbauer analysis showed that most of Fe^{2+} ions were in the low spin state S = 0, supporting the reduction of high spin Fe^{3+} ions to low spin Fe^{2+} ones beyond $z = 2.744$.

The small potential difference between the reduction and oxidation processes in the higher potential region around 0 V in Fig. 5 would result from fast oxygen diffusion in CLFO at the corresponding composition range, because the kinetics of electrode reactions involving insertion and extraction of a substance is usually controlled by the transport in a host material. Therefore, the chemical diffusion coefficient of oxygen was estimated by using a simple plane sheet diffusion model to be 1.2×10^{-13} cm^2 s^{-1} (see Fig. S3 in

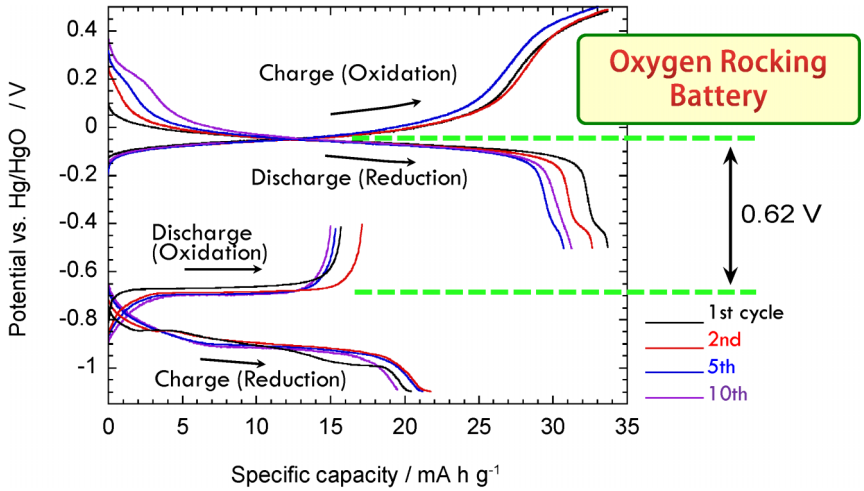

Figure 5 | The potential profiles of CLFO of redox repetition tests in the two different potential ranges at a constant current of 5.60 mA g^{-1}. The maximum capacities of the reduction and reoxidation processes in the potential region around −0.8 V were 20 and 15 mA h g^{-1}, respectively, and different from each other. This difference does not result from side reactions, but from the slow diffusion of oxygen, which would be overcome by fabricating a well-designed nano-structured electrode.

Supplementary Information). In comparison with the chemical diffusion coefficients of Li^+ ions in the typical LIB materials, the value is approximately a few to several orders of magnitude lower than those of $LiCoO_2$ (typically, 10^{-8} – 10^{-10} cm^2 s^{-1})[11–13] and $LiMn_2O_4$ (typically, 10^{-10} – 10^{-13} cm^2 s^{-1})[14–16] and one order of magnitude higher than that of $LiFePO_4$ (1.8×10^{-14} cm^2 s^{-1})[17]. Since the size of the oxygen ion is much larger than those of lithium, sodium, and magnesium ions, the diffusivity of the oxygen ion is generally lower than those of lithium, sodium, and magnesium ions. This low diffusivity would result in the operation of oxygen rocking batteries at lower currents.

In the lower potential region around −0.8 V, reduction and oxidation capacities are ca. 20 and 15 mA h g^{-1}, respectively, and much smaller than 70.2 mA h g^{-1} estimated on the assumption that the oxygen content ranges from 2.75 to 2.50 ($\Delta z = 0.25$). In the same potential region in Fig. 2, the oxygen content ranged from 2.75 to 2.53 ($\Delta z = 0.22$) and the Δz of 0.22 corresponded to 88% of the $\Delta z = 0.25$. Since the electrochemical reduction in Figs. 2 and 5 were conducted at 5.6 and 1.4 mA g^{-1}, respectively, the capacities around −0.8 V depended on current densities (see Fig. S3 in Supplementary information). This is likely explained by much slower oxygen diffusion (the estimated chemical diffusion coefficient; 1×10^{-15} cm^2 s^{-1}, see eq. S5 and discussion in Supplementary information). Such slow oxygen diffusion in this content range would be related to ordering of oxygen vacancies such as one dimensional arrangement of oxygen vacancies observed in the brownmillerite structure, since the formation of microdomains upon the appearance of the brownmillerite $CaFeO_{2.5}$ phase in $Ca_xLa_{1-x}FeO_{3-x/2}$ has been reported[18].

In conclusion, the electrochemical reduction of Fe^{4+} to Fe^{3+} and Fe^{3+} to Fe^{2+} and their reoxidation in CLFO proceed reversibly and repeatedly via extraction and reinsertion of oxygen in two potential regions around 0 V and − 0.8 V. This shows that CLFO can serve as both cathode and anode materials in an oxygen rocking battery. The CLFO is, however, one of model electrode materials of the oxygen rocking batteries, and the developments of more suitable materials for each of a cathode and an anode will enable the new practicable oxygen rocking batteries.

Methods

Powders of $Ca(CH_3COO)_2{\cdot}H_2O$ (0.881 g, 5.0 mmol), $La(CH_3COO)_3{\cdot}1.5H_2O$ (1.715 g, 5.0 mmol), $Fe(NO_3)_3{\cdot}9H_2O$ (4.040 g, 10.0 mmol), and citric acid monohydrate (4.203 g, 20.0 mmol) were dissolved in ultrapure water (80 mL). The solution was evaporated to dryness at 60°C followed by the evaculation at 100°C. The powder was ground with an agate mortar and calcined at 300°C in air followed by grounding. The powder was heated to 1000°C at 10°C min^{-1}, kept at 1000°C for 10 min and cooled to room temperature in a furnace. The average valences of iron ions was determined to be 3.226(2) by the iodometric titration and the empirical formula was $Ca_{0.5}La_{0.5}FeO_{2.863(1)}$.

The CLFO samples ($z = 2.827 - 2.618$) were prepared by electrochemical reduction of $Ca_{0.5}La_{0.5}FeO_{2.863}$ with three electrode glass cells.

The electrochemically-reduced CLFO samples were removed from the glass cells, mounted in air-tight sample holder in an inert gas system, and were structurally analyzed by X-ray diffractometry using monochromated Cu-Kα_1. The local conditions of iron ions were investigated by Mössbauer spectroscopy using ^{57}Co at room temperature. The parameters (the isomer shift relative to α-Fe (IS), the quadrupole splitting (QS), the internal magnetic field (B), and the relative intensity of the component (I)) were refined by profile-fitting (see Fig. S2 and discussion in Supplementary information). The oxygen contents in CLFO could be determined with the Mössbauer data in two ways: (1) The average valences of iron ions were calculated with the valences and relative intensities of the components, and the oxygen contents were determined. (2) The oxygen contents were calculated with the coordination numbers of the oxygen surrounding iron ions (tetrahedral, square-pyramidal and octahedral iron sites possess 2, 2.5, and 3 oxide ions, respectively.)

Electrochemical measurements were performed using a three electrode beaker cell with a reference electrode (Hg/HgO) and an electrolyte solution (1 M NaOH aq). A platinum mesh was used as a counter electrode. A mixture of CLFO, conducting additive (KS-6L, Timcal), and binder (PTFE powder) in the ratio 77/19/3 (w/w) was ground, pressed on a current collector, and used as a working electrode. A platinum mesh was employed as the current collector for oxidation and a gold one for reduction, because they have high overpotential of oxygen evolution and hydrogen evolution, respectively. The oxidation or reduction at a constant current ranging from 1.40 to 28.0 mA g^{-1} was performed to investigate the electrochemical behavior of $Ca_{0.5}La_{0.5}FeO_{2.863}$. The reversibility and repeatability were investigated by the redox tests at a constant current of 5.60 mA g^{-1} in the potential ranges 0.5 − −0.5 V and −0.4 − −1.1 V.

1. Ellis, B. L., Makahnouk, W. R. M., Makimura, Y., Toghill, K. & Nazar, F. A multifunctional 3.5 V iron-based phosphate cathode for rechargeable batteries. *Nat. Mater.* **6**, 749–753 (2007).
2. Wessells, C. D., Peddada, S. V., Huggins, R. A. & Cui, Y. Nickel hexacyanoferrate nanoparticle electrodes for aqueous sodium and potassium ion batteries. *Nano Lett.* **11**, 5421–5425 (2011).
3. Nakamura, E. & Sato, K. Managing the scarcity of chemical elements. *Nat. Mater.* **10**, 158–161 (2011).
4. Kudo, T., Obayashi, H. & Gejo, T. Electrochemical behavior of the perovskite-type $Nd_{1-x}Sr_xCoO_3$ in an aqueous alkaline solution. *J. Electrochem. Soc.* **122**, 159–163 (1975).
5. Van Buren, F. R., Broers, G. H. J., Bouman, A. J. & Boesveld, C. An electrochemical method for the determination of oxygen ion diffusion coefficients in $La_{1-x}Sr_xCoO_{3-y}$ compounds. Theoretical aspects. *J. Electroanal. Chem.* **87**, 389–394 (1978).
6. Takeda, Y., Okazoe, C., Imanishi, N., Yamamoto, O., Kawasaki, S. & Takano, M. Oxygen doping in $Ca_{1-x}Sr_xFeO_{3-z}$ perovskite oxides by an electrochemical method. *J. Ceram. Soc. Jpn.* **106**, 759–762 (1998).
7. Nemudry, A., Rogatchev, A., Gainutdinov, I. & Schöllhorn, R. Reactivity of the perovskite system $Ca_{1-x}Sr_xFeO_{2.5}$ in topotactic electrochemical oxidation at ambient temperature. *J. Solid State Electrochem.* **5**, 450–458 (2001).
8. Longo, J. M., & Clavenna, L. R. Use of perovskites and perovskite-related compounds as battery cathodes. *U.S. Patent* US 3939008 (1976).
9. Wattiaux, A., Grenier, J. C., Pouchard, M. & Hagenmuller, P. Electrolytic oxygen evolution in alkaline medium on $La_{1-x}Sr_xFeO_{3-y}$ perovskite-related ferrites. I. Electrochemical study. *J. Electrochem. Soc.* **134**, 1714–1718 (1987).
10. Shannon, R. D. Revised effective ionic radii and systematic studies of interatomic distances in halides and chalcogenides. *Acta Cryst. A* **32**, 751–767(1976).
11. Thomas, M. G. S. R., Bruce, P. G. & Goodenough, J. B. Lithium mobility in the layered lithium cobalt oxide ($Li_{1-x}CoO_2$). *Solid State Ionics* **17**, 13–19 (1985).
12. Zhang, Y., Lu, Z. G., Chung, C. Y., & Zhu, M. Kinetics of Li^+ transport and capacity retention capability of HT-$LiCoO_2$ films. *Physica Scripta T* **129**, 38–42 (2007).
13. Cao, Q. *et al.* A novel carbon-coated $LiCoO_2$ as cathode material for lithium ion battery. *Electrochem. Commun.* **9**, 1228–1232 (2007).
14. Shih, F. -Y. & Fung, K. -Z. Effect of annealing temperature on electrochemical performance of thin-film $LiMn_2O_4$ cathode. *J. Power Sources* **159**, 179–185 (2006).
15. Lu, D. S., Li, W. S., Zuo, X. X., Yuan, Z. Z. & Huang, Q. M. Study on electrode kinetics of Li^+ insertion in $Li_xMn_2O_4$ ($0 \le x \le 1$) by electrochemical impedance spectroscopy. *J. Phys. Chem. C* **111**, 12067–12074 (2007).
16. Chung, M. -D., Seo, J. -H., Zhang, X. -C. & Sastry, A. M. Implementing realistic Geometry and Measured Diffusion Coefficients into Single Particle Electrode modeling based on experiments with single $LiMn_2O_4$ spinel particles. *J. Electrochem. Soc.* **158**, A371–A378 (2011).
17. Prosini, P. P., Lisi, M., Zane, D. & Pasquali, M. Determination of the chemical diffusion coefficient of lithium in $LiFePO_4$. *Solid State Ionics* **148**, 45–51 (2002).
18. Vallet-Regí, M., González-Calbet, J., Alario-Franco, M. A., Grenier, J. C. & Hagenmuller, P. Structrual intergrowth in the $Ca_xLa_{1-x}FeO_{3-x/2}$ system ($0 \le x \le 1$): An electron microscopy study. *J. Solid State Chem.* **55**, 251–261 (1984).

Acknowledgment

This research is supported by the Japan Society for the Promotion of Science (JSPS) through its "Funding Program for World-Leading Innovative R&D on Science and Technology (FIRST Program)".

Author contributions

M.H. designed the study in collaboration with N.M. and performed the Rietveld refinement and Mössbauer analysis; Y.S. performed the synthesis and chemical characterizations; T.Kimura conducted electrochemical measurements and Mössbauer experiments; All the authors discussed the results; M.H. and N.M. wrote the manuscript, with comments from T.Kudo.

Additional information

Supplementary information accompanies this paper at http://www.nature.com/scientificreports

Competing financial interests: The authors declare no competing financial interests.

How to cite this article: Hibino, M., Kimura, T., Suga, Y., Kudo, T. & Mizuno, N. Oxygen rocking aqueous batteries utilizing reversible *topotactic* oxygen insertion/extraction in iron-based perovskite oxides $Ca_{1-x}La_xFeO_{3-\delta}$. *Sci. Rep.* **2**, 601; DOI:10.1038/srep00601 (2012).